Onset-Triggered Vote-Locking (OTVL) for Stable Myoelectric Control of Multi-DoF Prosthetic Hands

Alessandra Pero, Erik Gasparini, Tommaso Mori, Cristian Felipe Blanco-Diaz, *Graduate Student Member, IEEE*, Rodolfo Cerqueira, Waleed Al-Ghilan, Sophie Skach, Leonardo Cappello, *Senior Member, IEEE*, Enzo Mastinu, *Senior Member, IEEE*, and Christian Cipriani, *Senior Member, IEEE*

***Abstract*— This study presents a novel semi-locked myoelectric pattern recognition algorithm (Onset-Triggered Vote-Locking or OTVL) to reduce misclassifications that typically occur during transition phases of muscular contractions for prosthetic hand control. It segments the electromyographic signals in real-time by adaptively defining enabling and disabling conditions at the onset of a muscular contraction in order to lock classifier predictions only when they are considered stable. The segmentation is based on signal standard deviation to improve robustness and reduce the need for rest transitions between movements. The proposed algorithm was implemented with a standard Linear Discriminant Analysis (LDA). It was functionally assessed by simulating activities of daily living and compared against a continuous LDA classifier with two conventional post-processing algorithms: Majority Vote (MV) and Confidence Rejection (CR). Eleven able-bodied participants executed ten repetitions of three Southampton Hand Assessment Procedure (SHAP) tasks using a bypass socket equipped with an active wrist and a multi-articulated hand. The OTVL algorithm significantly outperformed CR in terms of success rate (median:IQR; OTVL: 100.0%:0%; CR: 10.0%:60.0%; $p < 0.001$). Compared to MV, OTVL significantly reduced total completion time (OTVL: 56.4s:20.6s; MV: 62.2s:7.7s; $p < 0.05$) and the number of incorrect preshapes (OTVL: 0.6:0.4; MV: 1.5:1.3; $p < 0.01$) that occurred between tasks. The perceived workload, as assessed by the NASA Task Load Index, was also significantly reduced compared to MV and CR (OTVL: 52:33.5; MV: 67:21.5; CR: 95:36.3; $p < 0.001$). Therefore, the OTVL algorithm represents a viable alternative to traditional continuous classifiers, improving control stability and task execution.**

***Index Terms*— Event detection, myoelectric control, pattern recognition, prosthetics, signal processing.**

Received 20 November 2025; revised 11 May 2026 and 24 June 2026; accepted 20 August 2026. Date of publication 3 September 2026; date of current version 14 September 2026. Associate Editor: Xiaogang Hu. This work was supported in part by Italian Ministry of University and Research under the Complementary Actions to NRRP through the "Fit4MedRob—Fit for Medical Robotics" under Grant PNC0000007 and through the "Young Researcher 2024" under Grant 0000057 and in part by INAIL within the framework of the NoProblem Project under Grant PR23-CR-P3. The work of Leonardo Cappello was supported by European Union (ERC, MUSE) under Grant 101116249. *(Alessandra Pero and Erik Gasparini are co-first authors.) (Corresponding author: Enzo Mastinu.)*

This work involved human subjects or animals in its research. Approval of all ethical and experimental procedures and protocols was granted by the Local Ethical Committee of the Scuola Superiore Sant'Anna, Pisa, Italy, under Application No. 10/2023, and performed in line with the Declaration of Helsinki.

The authors are with the BioRobotics Institute and the Department of Excellence in Robotics and AI, Scuola Superiore Sant'Anna, 56127 Pisa, Italy (e-mail: enzo.mastinu@santannapisa.it).

This article has supplementary downloadable material available at https://doi.org/10.1109/TNSRE.2026.3730074, provided by the authors.
Digital Object Identifier 10.1109/TNSRE.2026.3730074

I. Introduction

MYOELECTRIC upper limb prosthetics hold a wide potential to restore user independence. However, their control still represents a major challenge for users [1], leading to consistently high abandonment rates [2]. The most widespread control technique is Amplitude and Threshold Control or Direct Control (DC), in which a pair of sensors decode electromyographic (EMG) signals from a pair of agonist-antagonist residual muscles. This control can be extended to multiple Degrees of Freedom (DoF) through myoelectric switching strategies (e.g., hold open or co-contraction) that cyclically select the desired DoF. Although straightforward and robust, this method hardly scales with increasing DoFs or more complex tasks [3]. Pattern Recognition (PR) techniques, instead, aim to improve the intuitiveness and reliability of prosthetic control by decoding user intention, based on the assumption that different desired movements correspond to different and repeatable EMG patterns. After the pioneering work of Wirta et al. [4], Englehart et al. first implemented a continuous classifier that inferred user intention from a constant stream of sliding EMG windows, with latencies short enough to be perceived as in real time [5], [6]. Since then, continuous classifiers have dominated the literature, demonstrating a broader use of grips in unsupervised environments [7], with systems based on this technology that progressively reached commercialization [8], [9], [10]. However, several sources of interference can limit PR reliability, such as arm posture [11], [12], [13], electrode repositioning [14], and muscle fatigue [15]. Classifiers trained only on the steady-state portion of the muscular contractions are particularly prone to errors in the transient portions [16]. For instance, Linear Discriminant Analysis (LDA) classifiers assume that the classes follow Gaussian mixture distributions, an assumption that is typically violated in the transition phases of a muscular contraction. Although the stream of independent predictions guarantees responsiveness and revisability of wrong prosthetic outputs, it may lead to isolated mispredictions [6]. To minimize the impact of these errors, various post-classification algorithms–essentially low-pass filters on the prediction - have been developed, such as the Majority Vote (MV) [6], Ramp [17], and Confidence-based Rejection (CR) [18].

Unlike continuous classifiers, locked predictors aim at enhancing control stability by holding the classifier prediction constant during the muscular contraction [19]. To lock the classifier predictions, the EMG waveform is usually "segmented" by the definition of locking and unlocking criteria. Transient algorithms, for example, lock the prediction by decoding the onset of the muscular contraction and usually unlock when the EMG intensity decreases to rest levels (EMG offset) [19], [20], [21], [22]. This framework simplifies the control problem by eliminating the need for an explicit rest class definition. Furthermore, the onset of a muscular contraction anticipates the steady-state phase [19], [20], [23], and has been demonstrated to include relevant content to estimate grasp force [24], [25], [26], grasps [20], and hand and wrist movements [21], [22], [27]. However, transient algorithms require intensive training for the user because only one sample is extracted for training the model, for each movement repetition [21], [22]. Moreover, if a misprediction occurs, the user must return to a rest state before re-attempting the movement [20], [21].

To combine the unconstrained revisability of continuous classifiers with the stability of locked predictors, Zhang et al. [28] proposed a hybrid semi-locked approach. This method detected the onset of a muscular contraction, collected EMG signals for 600 ms, and then locked predictions to the most voted class in this time interval. They proposed different onset approaches, including one based on the EMG Mean Absolute Value (MAV), and one based on the Teager-Kaiser Energy Operator (TKEO). They compared them to a conventional continuous classifier and to its variant with Majority Vote. Eight unimpaired participants plus two transradial amputees participated in a virtual task that involved six active movements and demonstrated semi-locked algorithms outperforming their continuous counterparts.

These promising results were later questioned by Raghu et al., who found that a MAV-based semi-locked method significantly underperformed when compared with continuous classifiers and post-processing algorithms [29]. Their work involved 43 able-bodied participants performing rapid transitions among six hand and wrist movements, following a visual computer prompt. The poor performances were associated with the dynamic nature of the task, in which movements were not followed by rest periods, i.e., the usual offset condition of locked and semi-locked predictors. Indeed, the need for a rest state was the claimed reason why Englehart and Hudgins moved from transient algorithms to continuous classifiers [5], [6], and proved to be a limiting factor of following locked predictors [22], [28].

Building on these early studies, in this work, we propose a novel semi-locked algorithm (Figure 1), namely Onset-Triggered Vote-Locking (OTVL) algorithm applied to a traditional LDA classifier, to improve prosthetic control by reducing misclassifications that typically occur during the transition phases of a muscular contraction. The OTVL algorithm included a segmentation algorithm based on Standard Deviation (STD) peaks that adapts, at the onset of a contraction, the thresholds associated with the offset, and the onset of possible following fast contractions. Then, a *Decision Algorithm* locks the classifiers' outputs once the predictions of the LDA are considered stable, thereby minimizing erroneous transitions between states. We hypothesized that this mechanism would result in a significant improvement in prosthetic control and a reduction in misclassifications, compared to traditional continuous classifiers (LDA) with standard post-processing (MV and CR). To quantify these improvements, we evaluated success rate, total completion time, number of incorrect preshapes, and NASA Task Load Index (NASA-TLX) perceived workload from eleven participants while performing activities of daily living of the Southampton Hand Assessment Procedure (SHAP). This served as a preliminary step, although further experimentation must be conducted with the target population to reach clinical validation. The OTVL algorithm significantly outperformed CR in terms of success rate (median:IQR; OTVL-100.0%:0%; CR-10.0%:60.0%; $p < 0.001$). Furthermore, the OTVL significantly reduced the median total completion time by ~9% (OTVL-56.4s vs. MV-62.2s; $p < 0.05$) and the median number of incorrect preshapes by 60% (OTVL-0.6 vs. MV-1.5; $p < 0.01$) relative to the Majority Vote approach, while also yielding the lowest perceived user workload (OTVL-52:33.5; MV-67:21.5; CR-95:36.3; $p < 0.001$).

II. Algorithm Description

The proposed *Onset-Triggered Vote-Locking* algorithm can be decomposed into two sub-algorithms. The *Segmentation Algorithm* identifies locking and unlocking criteria, while the *Decision Algorithm* determines the final prediction based on the temporal evolution of the continuous classifier stream. To describe the algorithm, we first define the relevant terminology. Let $EMG \in \mathbb{R}^{N_s x C x M x R}$ be the EMG dataset used for calibrating the OTVL algorithm, where N_s is the number of samples, C is the number of channels, M is the number of movements, and R is the number of repetitions. During each movement (m) and repetition (r), the EMG signals corresponding to a muscular contraction beginning and ending in a rest state are recorded through conventional pre-amplified and rectifying myoelectric electrodes (Myobock, Ottobock, Germany). From this EMG dataset, $MAV \in \mathbb{R}^{N_{iTW} x C x M x R}$ and $STD \in \mathbb{R}^{N_{iTW} x C x M x R}$ are computed over sliding windows of the EMG signal (where N_{iTW} is the number of incremental time windows). Then, the average MAV ($aMAV \in \mathbb{R}^{N_{iTW} x M x R}$) and the average STD ($aSTD \in \mathbb{R}^{N_{iTW} x M x R}$) are computed across channels.

A. Segmentation Algorithm

To segment muscular contractions in real-time, a novel algorithm was developed by leveraging $aSTD$ peaks to derive a subject-specific threshold ($aSTD_{peak\ onset\ min}$) for detecting

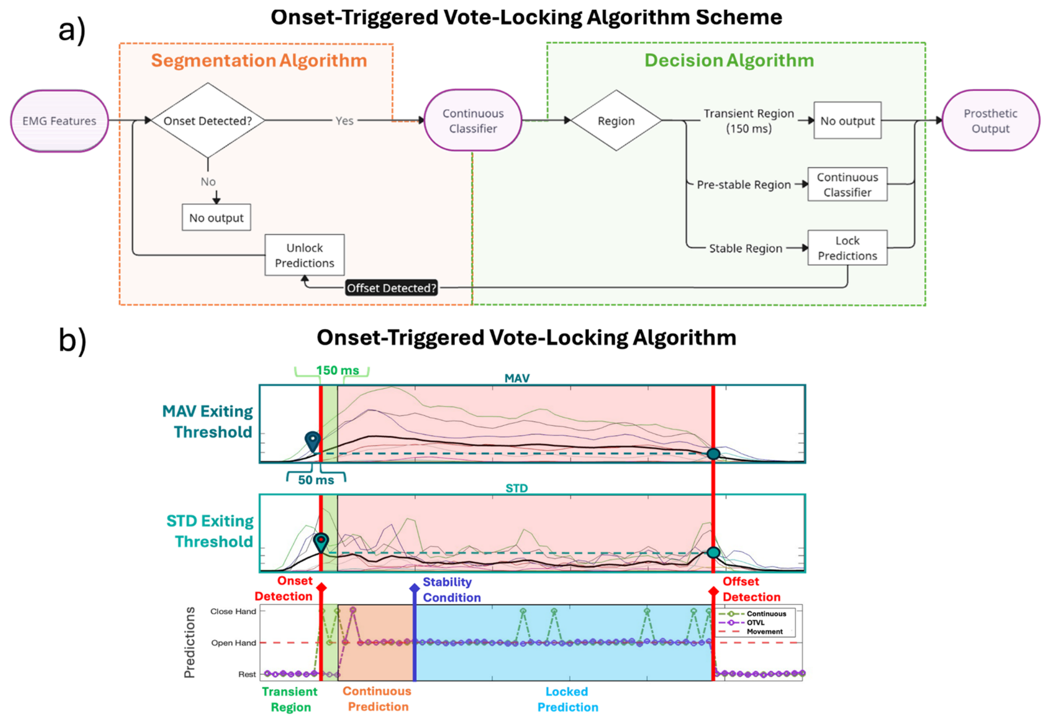

Fig. 1. Onset-Triggered Vote-Locking (OTVL) framework. a) OTVL Scheme: the segmentation algorithm determines muscular contraction onset and offset. If no onset is detected, a rest state is determined. Otherwise, the decision algorithm determines the output from the continuous classifier. Predictions within the transient region (150 ms after onset detection) are ignored. After this time interval, predictions are streamed continuously until the stability condition is met, defined as 8 consistent predictions out of the last 10. The corresponding class is then locked and maintained until the end of the muscular contraction or a new rapid movement are detected by the segmentation algorithm. b) Online implementation of the OTVL algorithm. The top two panels show the average Mean Absolute Value (aMAV) and average Standard Deviation (aSTD) signals with the detected onset and offset (orange vertical lines) and the conditions used to determine contraction termination. aMAV values lower than the aMAV threshold correspond to the end of the muscular contraction, while aSTD peaks greater than the aSTD threshold correspond to the start of a new movement. Colored curves represent MAV and STD from individual EMG channels, while the black line indicates the average across channels. The bottom panel shows the classification outputs of the OTVL, compared to a typical continuous classifier. Different predictions of the decision algorithm are highlighted with colored regions. The blue vertical line represents when the stability condition is determined.

the contraction onset. Indeed, sliding windows of signal variance, normalized by the variance computed during previous rest states, were shown to reliably detect EMG muscular contractions onsets [30], [31]. In the current implementation, $aSTD$ peaks were leveraged to remove the normalization from rest states, thus facilitating rapid transitions between movements.

The peaks of $aSTD$ were identified by sign changes in the first derivative of the $aSTD$ time series. Candidate peaks ($aST_{peak\ candidates,m,r}$) were selected based on the following conditions: (i) they occurred in the first half of the repetition, (ii) they were within a region where $aMAV$ was increasing (i.e., a positive derivative), and (iii) their amplitude exceeded six times the median $aSTD$ during rest, as in a similar onset detector [22], to minimize possible false positive detections. The earliest $aSTD_{peak\ candidates,m,r}$ in each repetition was selected as the $aSTD_{peak,m,r}$, while $aSTD_{peak\ onset\ min}$ was defined as the minimum of $aSTD_{peak,m,r}$ across all repetitions and movements, ensuring high sensitivity also for weaker EMG contractions [22]. This value served then as the reference threshold for detecting contraction onsets in both offline classifier training and real-time control. The global threshold was paired with the conservative amplitude threshold for identifying candidate onsets (six times the median $aSTD$ during rest) to balance robustness and movement detection.

A contraction was considered to begin (onset) at the first instance of a new peak of $aSTD$ that exceeded $aSTD_{peak\,onset\,min}$ (1) in a region of increasing $aMAV$, reflecting increased signal variability associated with muscle activation. The end of the contraction (offset), adapted for each muscular activation, was based on one of two alternative criteria, defined empirically from preliminary testing (Figure 1b). Either condition was sufficient to determine the end of the contraction. The first condition was satisfied when a subsequent $aSTD_{peak}$ exceeded the peak observed at the onset. This condition was consistent with either the termination of the contraction or the initiation of a new rapid movement without returning to a rest state. The second condition applied when the $aMAV$ fell below the $aMAV$ immediately preceding the onset, reflecting a return to a low-activity or resting state (2).

Onset:

$$
\begin{aligned}
& aSTD_{peak,n,j} > aSTD_{peak\_onset\_min} \quad \text{and} \\
& aMAV_{n,j} > aMAV_{n-1,j} \\
& \text{With} \quad n\text{: } 50\, ms\ control\ cycle\ \ j\text{:}EMG\ waveform
\end{aligned}
\tag{1}
$$

End:

$$
\begin{aligned}
& aSTD_{n,j} > aSTD_{n_{onset},j} \quad \text{or} \\
& aMAV_{n} < aMAV_{n_{onset}-1,j}
\end{aligned}
\tag{2}
$$

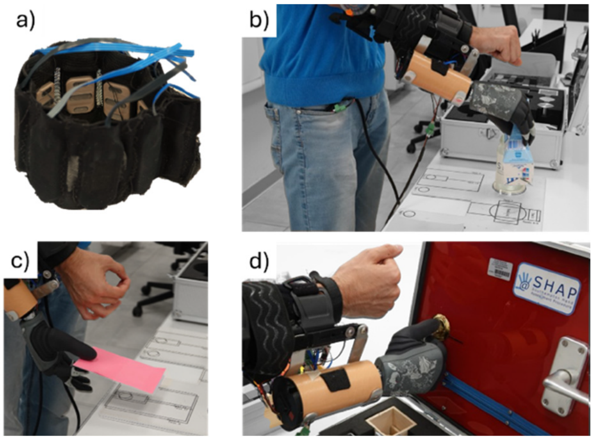

Fig. 2. Experimental setup to evaluate real-time prosthetic control. (a) Customized textile-based EMG bracelet of eight Myobock preamplified electrodes. (b, c, d) The three functional tasks used in the experimental protocol were selected from the Southampton Hand Assessment Procedure (SHAP). (b) Carton pouring (cylindrical grasp), (c) Page turning (pinch grasp), and (d) Rotate key (lateral grasp).

B. Decision Algorithm

Once an onset was detected, the EMG signal was classified in a continuous way, starting 150 ms after the onset to exclude the initial unstable portion of the EMG signal [20]. The predicted class was then locked once a *stability condition* was met. Similar to a majority-vote scheme that determines the output as the most frequent class among the last predictions [6], the *stability condition* was satisfied when 8 of the 10 most recent classifications were consistent. The locked prediction was then maintained until one of the offset criteria was met (Figure 1b).

III. Materials and Methods

A. Experimental Setup

The OTVL algorithm was compared against two alternative and consolidated post-processing methods: Majority Voting (MV) and Confidence Rejection (CR), frequently employed as benchmarks [29]. A standard LDA continuous classifier, commonly adopted as a robust baseline in myoelectric control due to its computational efficiency and proven performance in unsupervised environments [32], was used. It served as a consistent baseline to compare the three algorithms (OTVL, MV and CR) without confounding factors from exploiting different classifiers. The LDA was fed through features widely used in the field (MAV, Waveform Length, modified Zero Crossing, Slope Sign Change [3], [33]) extracted from 200 ms time windows with 150 ms overlap. STD was similarly extracted to train the OTVL *Segmentation Algorithm*. The MV was implemented over five decisions of the LDA continuous classifier (five windows) [17], which introduced a 150 ms delay between class transitions, as in the proposed OTVL implementation, thereby balancing classifier stability and user-perceived delay. CR was set with a 97% rejection threshold (lower estimated confidence resulted in the rest class), in alignment with previous literature evidence [18], [29], [34], [35].

The test was conducted on 11 able-bodied participants enrolled by convenience sampling (age 26.3 ± 1.8, 4 females, 10 right-handed). All participants gave their informed consent to participate in the study, according to the Declaration of Helsinki. The study was approved by the local ethical committee of the Scuola Superiore Sant'Anna, Pisa, Italy (ref. 10/2023). Eight commercial Myobock electrodes were placed around the participant's forearm in a cuff configuration using a custom-made elastic band. The band was placed 2 cm distal from the epicondyle, trying to avoid the ulnar bone with the electrodes. The elastic band was realized with a modular design, alternating 3D-printed solid cases for housing the EMG electrodes with elastic textile segments to secure wearing comfort and adaptability (Figure 2a). EMG samples were acquired through a custom device [33] at 1000 Hz, transmitted through Bluetooth, and labelled on the connected computer (CPU: 11th Generation Intel Core i7-11700 2.50 GHz, RAM: 32 GB). Each participant performed the experiment using a custom prosthesis bypass, simulating a transradial amputation. For this, participants wore an orthopaedic arm brace adapted to hold a prosthetic wrist (Electric Wrist Rotator, Ottobock, Germany) and a multi-articulated prosthetic hand (MIA Hand [36], Prensilia, Italy). This adapter allowed the free motion of the intact wrist and hand, while giving the possibility to block the elbow to reduce the forearm load. The combined weight of the bypass adapter and transradial prosthesis prototype was approximately 1.5 kg. The prosthetic components allowed participants to perform six movements: two wrist movements (wrist pronation and wrist supination), and four hand motions. Among them, there were three grasps (cylindrical, pinch, and lateral), and an open movement that opened the current grasp. The MAVs of the EMG signals of each movement were visually inspected, and the gain of each channel was software-adjusted to maximize class separability. All procedures were executed using a custom interface programmed in MATLAB 2023b.

B. Recording Session

For each of the six movements under test, the maximum voluntary contraction (MVC) and a calibration dataset were collected. The latter included three sessions at different arm height angles (with the elbow flexed at 45°, 90°, 135°) to improve robustness against arm position changes [13]. Each session included two repetitions of 5 s of contraction and 1 s of rest for each of the six movements. The participants were asked to perform gestures that mimicked prosthetic hand preshapes and wrist rotation. In particular, they performed a fist contraction for the cylindrical grasp, a tridigital grasp for the pinch grasp, a thumb up contraction for the lateral grasp, a palm-down for wrist pronation, and a palm-up for wrist supination (Figure 3).

During the procedure, the *aMAV* from all EMG channels was displayed to the participants as a biofeedback signal during the training. More in detail, the *aMAV* was displayed as a moving line plot showing the percentage of current signal intensity between rest and the MVC (0-100% intensity) of that specific movement. The participants were asked to follow

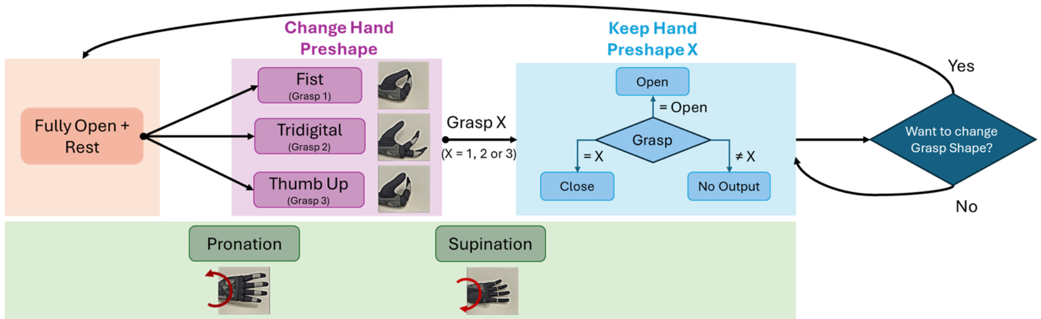

Fig. 3. Prosthesis operation (consistent across control algorithms). Once the prosthetic hand is in a specific preshape, a classifier prediction incoherent with that preshape does not provide a prosthetic output. To change the grasp, it is necessary to fully open the current grasp and rest. After this condition, one grasp prediction is sufficient to change the hand preshape.

with their *aMAV* a trapezoidal ramp displayed on the screen. The reference shape was composed of a rest phase (5% at the beginning and 5% at the end), a ramp-up phase (30%), a static contraction phase at 70% of the MVC (40%), and a ramp-down phase (20%).

C. Training of the Classifiers

The LDA classifier combined with the MV and CR was trained with a conventional data-cropping [37], [38]. This technique aimed to remove any transitory portion in the EMG, maximize the separability between rest and movement contractions, and ultimately comply with the Gaussian mixture distributions hypothesis. For this, 35% and 25% of EMG were removed from the beginning and the end of each movement recording, respectively. Instead, the LDA classifier combined with our OTVL algorithm was trained with only movement data directly provided by the proposed *Segmentation Algorithm*, thus from EMG samples extracted between the detected onset and offset. To address the consequent class imbalance caused by the *Segmentation Algorithm* that does not guarantee uniform sizes across classes, the Synthetic Minority Oversampling Technique (SMOTE) was applied to OTVL LDA [39], whereas the fixed trim percentage guaranteed class balance for the reference algorithms.

D. Assessment Procedure

A modified version of the Southampton Hand Assessment Procedure (SHAP [40]) was employed to compare the performance of the three controllers. The test was similar in structure to that used in [41], and consisted of three grasp-related tasks that also required wrist involvement: Carton Pouring (cylindrical grasp, Figure 2b)), Page Turning (pinch grasp, Figure 2c)), and Rotate Key (lateral grasp, Figure 2d)) (S1). The SHAP test is commonly used to assess upper limb prostheses, and its performance metrics are based on the execution time of a set of tasks (the faster, the better) [7], [42], [43], [44]. The time for hand preshaping and the wrist prepositioning are not explicitly included in the original test protocol, allowing off-timer adjustments before starting each task. However, here, we deemed these times of interest and thus we allowed preshaping and prepositioning only at the beginning of each sequence (i.e., once every three tasks).

Each participant performed 10 repetitions per algorithm, with 1-2-minute breaks between repetitions to minimize muscular fatigue. Additionally, they were allowed to test the full task sequence once with each algorithm before the formal evaluation. The order of both the tasks and the algorithms was pseudo-randomized within each repetition to minimize learning bias and muscular fatigue effects. Participants were blinded with respect to the control algorithm, although all conditions (OTVL, MV, CR) were clearly explained at the beginning of the experiment.

E. Prosthesis Operation

During the execution of the modified SHAP, the prosthesis operation was consistent across control algorithms (Figure 3). The switch among grasps was activated only if the current grasp was fully opened and after a rest classification. During grasp transitions (around 1 s), the output of the classifiers was ignored by the prosthesis to avoid conflicting preshape commands that could damage the device. This scheme balanced the potential desire to remain in a grip even if the hand was fully open, similar to the scheme used by Simon et al. [7], prioritizing user control. Indeed, our primary goal was to minimize erroneous grasp switching, since an unintended grip change during a task could be disruptive to the user experience. Within a specific preshape, a classifier prediction coherent with the current preshape allowed closing the current grasp, while an incoherent prediction did not produce a prosthetic output. The speed of each prosthetic movement was set proportionally to the EMG channel with the highest Signal-to-Noise Ratio (with respect to the rest state), recorded during training [33]. For example, if channel 1 resulted in the strongest Signal-to-Noise Ratio EMG during the “Wrist Pronation” training, then an amplitude of the same channel equivalent to the MVC would result in 100% speed of pronation, while lower values would be mapped proportionally.

To summarize real-time operation: EMG samples were collected in 200 ms windows with 150 ms overlap, yielding an LDA prediction every 50 ms, approximately 3 ms after data acquisition, processing, and feature classification [33]. CR introduced no additional delay. MV introduced a 150 ms delay between class transitions (including the rest class). OTVL introduced a fixed 150 ms delay after detection of a relevant STD peak; during this period, predictions were ignored. Immediately after, the prosthesis moved according to the continuous LDA predictions every 50 ms. In parallel, the OTVL algorithm monitored the prediction stream. Once 8 out of the last 10 predictions were consistent (a minimum observation of 400 ms), the output was locked (Figure 1b). This locking did not impose any additional user-perceived delay, because the prosthesis was already responding to the continuous stream. Instead, the lock was designed to primarily stabilize the end of contractions, where muscular fatigue and EMG offset might otherwise cause misclassifications, without compromising real-time responsiveness.

F. Metrics

For each repetition and participant, the total completion time (TCT) for the three-task sequence, the completion time of each individual task (CT), and the number of incorrect preshape (IP) activations were recorded. TCT and CT were tracked using a digital timer that the experimenter pressed at the beginning and end of each task, while the IP was determined as the count of wrong hand preshape transitions in the change from one task to the following, regardless of the control algorithm. For each metric, the representative value for each participant was computed as the average across the repetitions. Moreover, a repetition was considered successfully completed if the participant was able to complete all three tasks (carton pouring, page turning, and rotate key) within a time limit of 50 s per task. This time limit was established by halving the traditional SHAP threshold for each unsuccessful task execution (100 s) to minimize participants' fatigue [45]. If any task exceeded the time limit, the trial was interrupted and considered failed. Based on this, the success rate (SR) was defined for each participant as the percentage of completed trials. CT, TCT and IP were computed only considering completed trials. Indeed, they were not recorded for interrupted sequences, as they were not comparable with completed trials. However, their impact is reflected in the SR metric, which mitigates the risk of bias in the overall comparison. To assess potential learning effects across task repetitions, a linear mixed-effects model was fitted with the TCT of each repetition.

Furthermore, to investigate whether the hand and wrist prepositioning influenced single-task performances, the CT was differentiated among the trials when prepositioning was allowed (1st task) or not (2nd and 3rd).

Finally, to assess and compare the subjective perception of the different control strategies, participants completed the NASA-TLX questionnaire at the end of the 10 repetitions. The perceived workload (PW) score was computed as the sum of the scores across the six NASA-TLX questions [46], [47].

G. Statistical Analysis

All statistical analyses were performed in MATLAB R2023b (MathWorks, US) using built-in statistical functions. Data normality distribution was assessed using the Shapiro–Wilk test. A non-parametric Friedman test was used to analyze differences across repeated measures in the case of non-normal distributions. When significant main effects were detected, post hoc pairwise comparisons were conducted using the Wilcoxon signed-rank test with Bonferroni correction for multiple comparisons. Wilcoxon signed-rank tests were additionally used for paired comparisons between experimental conditions. Linear mixed-effects models were used to assess the effect of repetition while accounting for inter-subject variability. The model included repetition as a fixed effect and participant as a random effect to account for inter-subject variability. A nominal significance level of $\alpha = 0.05$ was adopted for all statistical tests. Results are presented as median and interquartile range (IQR).

H. Offline Analysis

The 150 ms transient window was based on previous studies [20], and both the window length and the onset detector were verified and optimized in pilot studies. To further validate these design choices, the training distributions across all subjects, sessions, movements, and repetitions were analyzed a posteriori. Specifically, the grand-average $aMAV$ and $aSTD$ profiles were computed and compared against the reference trapezoidal shape.

Similarly, the training distributions from each participant were used as a post-hoc analysis to validate the data cropping before training the reference LDA classifiers. Specifically, a structured two-fold cross-validation was performed for each participant. Thus, the LDA classifier was trained for each fold using one of the two repetitions for each arm angle and using the other as the test set. We evaluated two training conditions: i) the LDA was trained on all data from the recorded contraction, including the ramp-up, steady-state plateau, and ramp-down phases; ii) the LDA was trained only on the steady-state plateau, after removing 35% from the start and 25% from the end of each contraction. To provide a nuanced view of performance, we segmented the test data into three distinct phases based on the intended trapezoidal contraction profile that participants were asked to follow: I) Rest phase: the period at the beginning and end of the trial, where participants were instructed to be at rest. Only rest predictions were counted as correct. II) Transient (ascending and descending) phases: the ramp-up and ramp-down phases, where the muscle activity is changing. Both rest and specific movement predictions were counted as correct. III) Steady-State (plateau) phase: the sustained contraction period. Only specific movement predictions were counted as correct.

I. Online Analysis

To further validate the *Decision Algorithm*, we analyzed participants' performance across SHAP repetitions to characterize pre-locking stability (and thus the locking duration) and to quantify locking benefits. For each segmented EMG waveform between detected onset and offset, we categorized contractions as: (a) shorter than the 8-sample locking criterion (i.e., insufficient length to achieve stability); (b) sufficiently long but failing to reach the stability condition before offset; or (c) those that reached the 8/10 stability condition. For each category, the classifier stability was computed considering as ground truth the mode over the available predictions (a) and (b), or the locked prediction (c).

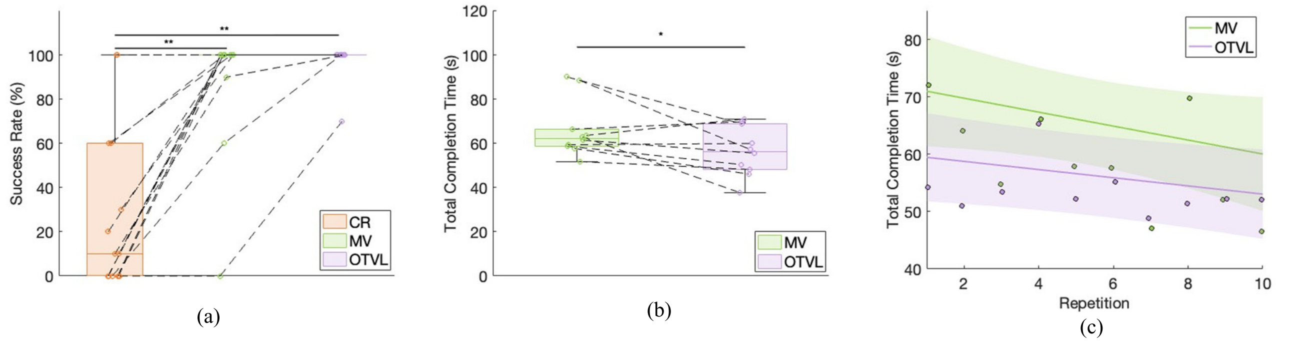

Fig. 4. Performance metrics across control strategies. a) Success rate: percentage of successfully completed trials within the 150 s threshold per task, compared across Confidence-based Rejection (CR), Majority Vote (MV), and the proposed Onset-Triggered Vote-Locking (OTVL). b) Total completion time (n = 10) of the completed trials: Time required to complete the full task sequence, compared between MV and OTVL. c) Linear mixed-effects model analysis of the Total Completion Time across repetitions for MV and OTVL. Solid lines represent fixed-effect trends; shaded areas indicate 95% confidence intervals. Dots represent the median total completion time across participants at each repetition for each algorithm. Boxplots are represented with median and IQR. Statistical significance is shown with "*" when $p < 0.05$ and "**" when $p < 0.01$.

A weighted overall stability was then computed for each repetition, considering the number of waveforms per category and their stability. For category (c), we also computed: (i) the stability of the pre-locking continuous stream, (ii) the time to lock the predictions, and (iii) the stability that the prosthesis would have executed without locking (i.e., considering only the LDA predictions). Results were averaged among the repetitions for each participant.

IV. Results

The total time required to complete the evaluation was approximately 30 minutes per algorithm, resulting in a total experiment duration of about 2 hours, including the electrode placement, donning of the device, algorithm training, and assessment. Overall, participants achieved the most stable and efficient performance when using the OTVL algorithm. Compared with the other control strategies, OTVL enabled consistent task execution across all subjects, faster completion of the task sequence, fewer control errors, and lower perceived workload. All distributions resulted in non-normality. Detailed results for each outcome measure are presented below.

A. Objective Metrics

1) Success Rate: The OTVL algorithm provided consistently reliable control (Figure 4a). All participants successfully completed the majority of trials under this condition, indicating robust and stable task execution. A similarly high level of consistency was observed with the MV algorithm, although performance showed slightly greater variability, and one participant was not able to complete any trial within the allowed timeout. Thus, for this participant, CT, TCT, and IP were not computed for any conditions (n = 10). In contrast, performance in the CR condition was markedly poorer: several participants were unable to complete the task sequence, resulting in substantially lower success rates. Quantitatively, the median success rate was 100% (IQR = 0%) for both OTVL and MV, compared to only 10% (IQR = 60%) for CR. The effect of the control strategy on success rate was statistically significant ($p < 0.001$). Post hoc analyses confirmed that both OTVL and MV achieved significantly higher success rates than CR ($p < 0.001$), whereas no difference was found between OTVL and MV ($p > 0.05$). Statistical comparisons involving the other objective metrics for CR were not conducted due to the limited number of successful trials with CR.

2) Total Completion Time: Task execution was faster when participants used the OTVL algorithm. On average, participants completed the three-task sequence more rapidly with OTVL than with MV, indicating more efficient execution of coordinated movements (Figure 4b). Median total completion time was 56.4 s (IQR = 20.6 s) for OTVL and 62.2 s (IQR = 7.7 s) for MV. This reduction in execution time was statistically significant ($p < 0.05$).

3) Learning Effect: Across repeated trials, a mild learning effect was observed for both OTVL and MV (Figure 4c). With OTVL, participants showed a gradual reduction in total completion time over the 10 repetitions, corresponding to an estimated slope of −0.71 s per repetition. A similar but slightly steeper trend (−1.22 s per repetition) was found with MV. Although these linear fits did not reach statistical significance (OTVL: $p = 0.058$, $R^2 = 0.50$; MV: $p = 0.083$, $R^2 = 0.18$), the downward trend suggests that both control strategies supported a modest degree of motor adaptation over time.

4) Task Completion Time: When using OTVL, participants executed individual tasks more rapidly when hand and wrist pre-positioning was possible, corresponding to the first position in the task sequence (Table I). The same pattern was observed with MV, indicating that pre-positioning facilitated execution for both control strategies (Table I). Statistical analysis confirmed a significant effect of task sequence position for both OTVL and MV ($p < 0.001$). For each algorithm, tasks performed in the first position were completed significantly faster than those in the second and third positions ($p < 0.01$), whereas no significant difference was observed between the second and third positions.

5) Incorrect Preshape Count: Participants made fewer incorrect preshape activations when using OTVL compared with MV, indicating more precise control and fewer unintended activations (Figure 5a). The median number of incorrect activations was 0.6 (IQR = 0.4) for OTVL and 1.5 (IQR = 1.3)

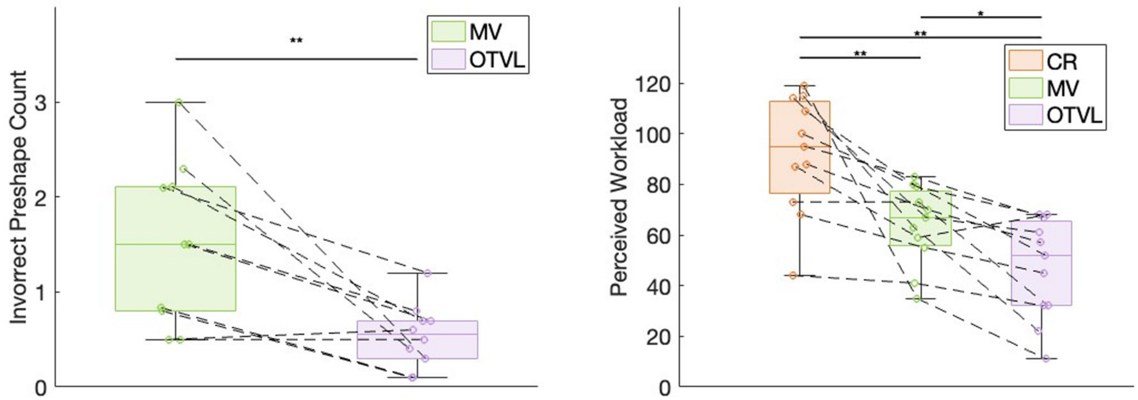

Fig. 5. Incorrect preshape count and perceived workload evaluation across control strategies. a) Incorrect preshape count (n = 10) of the completed trials, compared between Majority Vote (MV), and the proposed Onset-Triggered Vote-Locking (OTVL). b) Perceived workload: Overall NASA-TLX scores reported by participants for each strategy (Confidence-based Rejection (CR), MV, OTVL). Boxplots are represented with median and IQR. Statistical significance is shown with "*" when p < 0.05 and "**" when p < 0.01.

TABLE I

MEDIAN AND INTERQUARTILE RANGE (IQR) OF TASK COMPLETION TIMES (IN SECONDS) ACCORDING TO INDIVIDUAL TASKS (CARTON POURING, PAGE TURNING, ROTATE KEY) AND FOR ALL TASKS COMBINED (ALL TASKS). VALUES ARE SHOWN FOR EACH ALGORITHM AND TASK POSITION (1ST WHEN REPOSITION WAS ALLOWED, AND 2ND AND 3RD WHEN REPOSITION WAS NOT ALLOWED) USING THE FORMAT MEDIAN: IQR

Task Position	*Carton Pouring (s)*	*Page Turning (s)*	*Rotate Key (s)*	*All Tasks (s)*
		OTVL		
1^{st}	**11.9** : 3.6	**9.9** : 3.1	**11.3** : 3.7	**12.0** : 3.2
2^{nd}	**20.2** : 6.2	**23.2** : 7.7	**23.2** : 13.5	**23.3** : 6.3
3^{rd}	**20.5** : 7.8	**19.2** : 3.4	**22.0** : 5.6	**20.2** : 7.6
		MV		
1^{st}	**13.0** : 7.1	**12.0** : 2.1	**10.6** : 1.9	**13.0** : 3.6
2^{nd}	**24.6** : 25.5	**21.5** : 4.7	**25.1** : 10.6	**24.1** : 13.2
3^{rd}	**31.2** : 13.8	**19.8** : 6.7	**24.2** : 18.1	**26.2** : 6.0

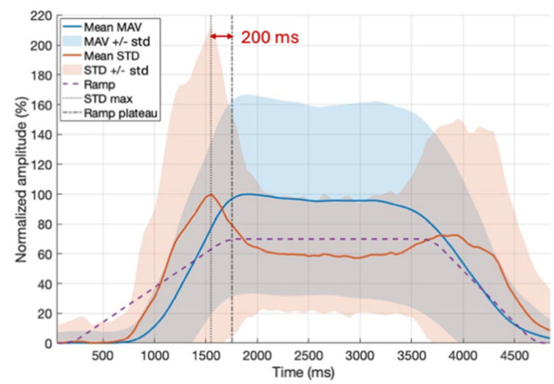

Fig. 6. Ensembled grand average of the normalized (as percentage) *aMAV* (blue) and *aSTD* (orange) across all participants, sessions, movements, and repetitions, with the trapezoidal visual prompt (violet). The shadows represent the standard deviation. The vertical straight line marks the detected *aSTD* peak, which occurs, on average, 200 ms before the ramp plateau (highlighted with a dashed vertical line).

for MV. This reduction in activation errors with OTVL was statistically significant ($p < 0.01$).

B. Subjective Metrics

1) Perceived Workload: OTVL was also associated with a lower perceived workload compared with the other control strategies (Figure 5b). Median NASA-TLX scores were 52 (IQR = 33.5) for OTVL, 67 (IQR = 21.5) for MV, and 95 (IQR = 36.3) for CR, indicating that OTVL required less cognitive and physical effort than MV and CR. Differences were statistically significant: post-hoc comparisons showed that workload with OTVL was significantly lower than with MV ($p < 0.01$) and CR ($p < 0.001$), and that workload with MV was significantly lower than CR ($p < 0.01$).

TABLE II

LDA CLASSIFICATION ACCURACY (MEAN ± STD) [%] ON DIFFERENT PHASES OF THE TEST DATA, WHEN TRAINED ON EITHER THE FULL CONTRACTION OR THE CROPPED, STEADY-STATE PORTION. FOR THE REST PHASE, ONLY REST PREDICTIONS WERE COUNTED AS CORRECT; FOR THE TRANSIENT PHASES, BOTH REST AND CLASS-SPECIFIC PREDICTIONS COUNTED AS CORRECT; FOR THE STEADY-STATE, ONLY THE CLASS-SPECIFIC PREDICTIONS COUNTED AS CORRECT

Accuracy (Mean ± Std) [%]	*Rest Phase*	*Transient Phases*	*Steady-State Phase*	*Overall*
Full Data	***96.9 ± 12.5***	***91.3 ± 22.5***	***92.0 ± 19.1***	***93.4 ± 18.0***
Cropped Data	***99.0 ± 6.2***	***94.4 ± 23.5***	***91.8 ± 19.0***	***95.1 ± 16.2***

C. Offline Analysis

The peak of the $aSTD$ grand averaged across subjects, sessions, movements, and repetitions occurred, on average, 200 ms before the beginning of the plateau of the reference ramp (Figure 6). Thus, validating the onset detector and the choice of rejecting predictions for 150 ms after the detected onset.

The results of the offline analysis demonstrate that for the baseline LDA (which includes the Rest class), training on cropped, steady-state data is superior (Table II). It yields higher overall accuracy and, critically, more accurate classification during the Rest and Transient phases. This confirms our cropping strategy was optimal for the baseline.

D. Online Analysis

Across participants, a median of 45 EMG waveforms was segmented. Among these, a median of 2 waveforms (less than 5%) fell into category (b)–sufficiently long but failing to reach stability. The weighted overall stability of OTVL (accounting for all waveforms) was 91.03% (IQR: 4.52%). For waveforms that reached the stability condition (median: 29), (i) the median stability of the pre-locking continuous stream was 91.65% (IQR: 4.88%) with an average of 1 misprediction occurring before lock per contraction. (ii) The median locking window was 452 ms (IQR: 35 ms). Critically, the locking mechanism itself improved stability by 5.56%: locked stability was 92.45% (IQR: 6.94%), compared to (iii) 86.89% (IQR: 7.35%) of the continuous stream without locking.

V. Discussion

This study proposed a novel semi-locked algorithm for myoelectric prosthetic control that automatically segments muscular contractions and locks its predictions once a stability criterion is met. Its performance was evaluated and compared with a continuous classifier (LDA) with two common post-processing strategies (CR and MV) in a functional assessment that resembled activities of daily living. Eleven able-bodied participants performed ten repetitions of a sequence of tasks that involved hand and wrist movements (Cartoon Pouring, Page Turning, and Rotate Key).

A. Performance Comparisons

Our proposed semi-locked algorithm considerably outperformed the other two testing conditions (continuous LDA with MV and CR), arguably providing a more stable prosthetic control as confirmed by the high success rate and the lowest total completion time (Figure 4). We limited the comparison to these two robust and well-established post-processing strategies to maintain a controlled experimental design; evaluating further post-processing conditions (e.g., [29]) would have required additional effort for the participants ($\approx$ 30 minutes per algorithm), risking the exacerbation of confounding factors such as fatigue and learning effects. Therefore, our results support the conclusion that OTVL is a promising alternative to conventional LDA-based continuous classifiers with traditional post-processing algorithms, but do not claim general superiority for stable multi-DoF prosthetic control.

On the contrary, Confidence Rejection performed the worst. Indeed, unexpectedly, most of the participants struggled to complete the task sequence within the allowed timeout due to frequent unwanted movement rejections, which limited smooth prosthetic control [18]. The fixed rejection threshold of 97% confidence was selected based on previous work [18], [29], [34], [35]. However, these studies were conducted in offline or virtual assessments; therefore, this threshold did not likely consider possible variations in the classifier confidence caused by factors such as muscle fatigue. Probably, the use of online adaptive rejection thresholds would have improved CR robustness in real-life applications [29]. Furthermore, in the original paper by Scheme et al. [18], the LDA classifier was trained using all data from the ramp contraction, while in the tested implementation, only the steady-state portions were exploited.

Considering the MV post-processing, one participant was not able to perform any task due to continuous misclassifications. Others reported prosthetic instability during task execution due to continuous mispredictions. The MV buffer of five windows was based on previous studies [17], and to keep consistency with the 150 ms delay introduced by the OTVL algorithm. A longer MV buffer (e.g., 7-time windows) would have probably mitigated this instability at the cost of longer movement transition (i.e., 200 ms) [17], [48]. Similarly, the rejection of classifier predictions for 150 ms after onset determination was intended to prioritize movement stability over minimum response time, although close to the optimal controller delay of 100-125 ms [49]. As expected, performances improved with time for both OTVL and MV (Figure 4b), probably due to task learning [50], [51]. The lowest TCT, especially in the first repetitions, may also suggest that the proposed OTVL immediately benefits prosthetic control.

We argue that the modifications introduced to the original SHAP protocol (continuous sequence of actions) are more representative of activities of daily living because they include and record the time needed to reposition the prosthesis (Table I). However, these modifications limit direct comparison with the previous vast SHAP literature and are meaningful only with those that reported completion times of individual SHAP tasks. For instance, the results presented here align with the literature when a task was the first in sequence. Indeed, Resnik et al. [52] reported the time of page turning of the Jebsen Taylor Hand Function test of two participants with a transradial amputation at intervals of one hour. In the first hour of the training, participants completed the task, on average, in 13.06 s. Furthermore, Amsuess et al. [53] reported average completion times for carton pouring (14.66 s), page turning (9.47 s), and rotate key (4.61 s) in two individuals with transradial amputation. The increased completion time of the key rotation task observed in our experiment was likely due to the added torque resistance introduced by the prosthetic bypass.

As expected, the proposed OTVL resulted in a significant reduction of the incorrect preshapes (Figure 5a). This reduction may be related to a better handling of the transient portions of the EMG signal. Indeed, the switch among grasps was activated only when the current grasp was fully opened and after a rest classification. This choice was made to reduce erroneous switching while opening the hand, similar to Simon et al [7], prioritizing user control over raw speed. The overall improvement of prosthetic control is likely the main reason why the perceived workload assessed by the NASA-TLX index was the lowest with the presented algorithm (Figure 5b).

Theoretically, the brief observation period (8 / 10 time windows) to confirm the user's intent before locking might create an unstable control phase between onset detection and vote-locking, during which the output could rapidly fluctuate as new labels arrived. However, our experimental results suggest that it did not create problematic instability in practice. Specifically, only a small fraction (<5%) of sufficiently long contractions failed to reach the stability condition, and the pre-locking phase achieved high stability (91.65%) with a median of only one misprediction before lock. Thus, the *Decision Algorithm* did not significantly impact real-time usability, as the prosthetic device followed user intention correctly even during the pre-locking phase, while isolated mispredictions minimally impacted prosthetic control. Moreover, the locking criterion provided substantial benefit at the end of contractions, where muscular fatigue and EMG offset would otherwise introduce instability, as evidenced by the 5.56% stability drop without locking. These findings, together with the significant reduction in incorrect preshapes and the lower perceived workload observed with OTVL (Figure 5) indicate that this observation period effectively filters spurious misclassifications without adding significant cognitive burden. Similarly, the use of a global minimum ($aSTD_{peak\,onset\,min}$) for detecting muscular contractions might have increased sensitivity (and possibly false onsets). For this reason, it was paired with the conservative amplitude threshold for identifying candidate onsets (six times the median $aSTD$ during rest) to balance robustness and movement detection.

B. Benefits of the Proposed Framework

The most similar semi-locked approach available in the literature is the one proposed by Zhang et al. [28]. A direct performance comparison is hard to draw, as Zhang's algorithm was tested in a virtual environment. Nevertheless, our potential improvements can be listed here. Our implementation required a shorter onset (150 ms instead of 600 ms) and did not require a fixed time period to lock predictions but relied on the consistent prediction output, avoiding locking unstable prosthetic outputs. Finally, the proposed *Segmentation Algorithm* facilitated movement transitions without the rest constraint of Zhang's proposal, by leveraging the STD for both onset [54], [55] and offset conditions [31].

Compared with traditional methods with onset detection based on MAV thresholds, here, STD was leveraged to improve robustness to real-life noise sources [28], [29]. Indeed, if an electrode breaks, its unchanging output results in a null STD value, minimizing the risk of false onset detections. Interestingly, STD is suggested to be more robust to muscular fatigue due to the relative compensation of the increase in EMG amplitude and reduced frequency [15]. Other state-of-the-art onset detectors based on energy, such as the TKEO [56], were not considered here because of incompatibility with rectified and low-passed pre-amplified electrodes. Indeed, the very low frequency output of these electrodes would result in high TKEO values only in the proximity of the EMG peak. Although the presented *Segmentation Algorithm* was only tested with premplified Myobock electrodes, similar results are expected to be achieved for electrodes with equivalent bandwidth or with proper digital filtering [54], [57].

The training datasets were not matched across the proposed method and the comparators. Specifically, the compared methods were trained after removing 35% and 25% from the beginning and end of each trial, respectively [37], [38], while the developed method was trained on samples selected by the proposed *Segmentation Algorithm*. This asymmetry was necessary for the need of the traditional LDA to have an explicit rest class definition. Therefore, any transitory portions in the EMG were eliminated to maximize the separability between rest and movement contractions. This design choice is supported by the performed offline analysis (Table II), which represents the trimmed version as the optimal baseline. Although not directly quantifiable from the performed experiment, the broader training distribution could have impacted users' functional performances, the main objective of the study. Indeed, some groups suggested that including the transient portion in the training set could improve real-time performances [58], [59], [60], albeit resulting in a higher number of rest false positives [58] and false negatives [59]. We argue that the rest class mispredictions reported by these groups might be related to an increased overlap between rest and active classes' distributions after the inclusion of the transient portions. Therefore, we decided to include transient portions only in the presented algorithm, in which no explicit rest class for the classifier is provided during classifier training. If having access to a broader training distribution positively impacted user performance, that would constitute a crucial advantage of the proposed framework, which represents an effective alternative to automatically determine transient and steady-state portions (Figure 6). Indeed, traditional screen-guided training was shown to suffer from user temporal compliance with the screen prompts, leading to a decrease in offline [61] and online [62] performances. Similarly, timing issues were reported by Simon et al during unsupervised prosthesis-guided-training [7].

Finally, although we applied this method to improve the LDA performance, compared to traditional post-processing strategies, the framework is generalizable. Indeed, it can be integrated with other classifiers and sensing modalities, such as sonomyography [63] or myokinetic control [44], once a reliable onset is assessed.

C. Limitations and Future Work

This study is not free from limitations. First, the experiment employed a bypass prosthesis operated by able-bodied participants. This approach has been widely used in prosthetic research to preliminarily assess solutions via the emulation of upper-limb amputation [64]. Although similar performances are expected, considering the above comparison of completion time from the targeted demographic [52], [53], future investigations must include individuals with upper-limb amputations to reach clinical validation. Second, the algorithm requires sustained EMG activity after the onset to avoid premature offset detections. Although this requirement of prolonged and high EMG signals might seem restrictive, we argue that it is not a limiting factor. Indeed, modern prosthetic devices can cover their whole range of motion in less than a second [36], [65], and signals with a small signal-to-noise ratio are generally less reliable. Furthermore, future studies may fine-tune some OTVL parameters (e.g., the number of STDs that determine candidate peaks for the OTVL training or a short MV approach in the OTVL continuous stream to further enhance stability) or may investigate the benefits of individually tuned parameters that might account for inter-individual variability. Finally, future studies may integrate information from the onset portion of the signal into Bayesian estimators to support the continuous assessment of the steady-state part.

Acknowledgment

The authors would like to thank all who participated in the experiments. The views and opinions expressed are, however, those of the authors only and do not necessarily reflect those of European Union or European Research Council. Neither European Union nor the granting authority can be held responsible for them.

Competing Interests

Christian Cipriani is the founder of Prensilia s.r.l, a university spin-off that develops multi-articulated and sensorized robotic hands. All authors declare that this research was conducted in the absence of any commercial or financial relationships that could constitute a potential conflict of interest.

Supplementary Material

Videos related to functional tests are available as "S1_OTVL_SHAP_tasks".

References

[1] P. Borracci, R. Guachi, L. Paternó, I. Mannari, F. Napoleoni, and M. Controzzi, "Organizing and prioritizing user needs for upper limb prostheses," in *Proc. Int. Conf. Rehabil. Robot. (ICORR)*, May 2025, pp. 1139–1146, doi: 10.1109/ICORR66766.2025.11063034.

[2] S. Salminger et al., "Current rates of prosthetic usage in upper-limb amputees—Have innovations had an impact on device acceptance?" *Disability Rehabil.*, vol. 44, no. 14, pp. 3708–3713, Jul. 2022, doi: 10.1080/09638288.2020.1866684.

[3] S. Amsuess, P. Goebel, B. Graimann, and D. Farina, "A multi-class proportional myocontrol algorithm for upper limb prosthesis control: Validation in real-life scenarios on amputees," *IEEE Trans. Neural Syst. Rehabil. Eng.*, vol. 23, no. 5, pp. 827–836, Sep. 2015, doi: 10.1109/TNSRE.2014.2361478.

[4] R. W. Wirta, D. R. Taylor, and F. R. Finley, "Pattern-recognition arm prosthesis: A historical perspective—A final report," *J. Rehabil. Res. Dev.*, pp. 8–35, Jan. 1978, doi: https://app.dimensions.ai/details/publication/pub.1079878228

[5] K. Englehart, B. Hudgin, and P. A. Parker, "A wavelet-based continuous classification scheme for multifunction myoelectric control," *IEEE Trans. Biomed. Eng.*, vol. 48, no. 3, pp. 302–311, Mar. 2001, doi: 10.1109/10.914793.

[6] K. Englehart and B. Hudgins, "A robust, real-time control scheme for multifunction myoelectric control," *IEEE Trans. Biomed. Eng.*, vol. 50, no. 7, pp. 848–854, Jul. 2003, doi: 10.1109/TBME.2003.813539.

[7] A. M. Simon et al., "User performance with a transradial multi-articulating hand prosthesis during pattern recognition and direct control home use," *IEEE Trans. Neural Syst. Rehabil. Eng.*, vol. 31, pp. 271–281, 2023, doi: 10.1109/TNSRE.2022.3221558.

[8] COAPT. *Complete Control*. [Online]. Available: https://coaptengineering.com/

[9] Ottobock. *MyoPlus*. [Online]. Available: https://shop.ottobock.us/Prosthetics/Upper-Limb-Prosthetics/Myo-Plus/c/2901

[10] IBT. *Glide*. [Online]. Available: https://www.i-biomed.com/glide

[11] C. Cipriani, M. Controzzi, G. Kanitz, and R. Sassu, "The effects of weight and inertia of the prosthesis on the sensitivity of electromyographic pattern recognition in relax state," *JPO J. Prosthetics Orthotics*, vol. 24, no. 2, pp. 86–92, 2012. [Online]. Available: https://journals.lww.com/jpojournal/fulltext/2012/04000/the_effects_of_weight_and_inertia_of_the.8.aspx

[12] E. Scheme, A. Fougner, Ø. Stavdahl, A. D. C. Chan, and K. Englehart, "Examining the adverse effects of limb position on pattern recognition based myoelectric control," in *Proc. Annu. Int. Conf. IEEE Eng. Med. Biol.*, Aug. 2010, pp. 6337–6340, doi: 10.1109/IEMBS.2010.5627638.

[13] A. Fougner, E. Scheme, A. D. C. Chan, K. Englehart, and Ø. Stavdahl, "Resolving the limb position effect in myoelectric pattern recognition," *IEEE Trans. Neural Syst. Rehabil. Eng.*, vol. 19, no. 6, pp. 644–651, Dec. 2011, doi: 10.1109/TNSRE.2011.2163529.

[14] B. Milosevic, E. Farella, and S. Benatti, "Exploring arm posture and temporal variability in myoelectric hand gesture recognition," in *Proc. 7th IEEE Int. Conf. Biomed. Robot. Biomechatronics (Biorob)*, Aug. 2018, pp. 1032–1037, doi: 10.1109/BIOROB.2018.8487838.

[15] A. Ebied, A. M. Awadallah, M. A. Abbass, and Y. El-Sharkawy, "Upper limb muscle fatigue analysis using multi-channel surface EMG," in *Proc. 2nd Novel Intell. Lead. Emerg. Sci. Conf.* (NILES), Oct. 2020, pp. 423–427, doi: 10.1109/NILES50944.2020.9257909.

[16] T. Lorrain, N. Jiang, and D. Farina, "Influence of the training set on the accuracy of surface EMG classification in dynamic contractions for the control of multifunction prostheses," *J. NeuroEng. Rehabil.*, vol. 8, no. 1, p. 25, Dec. 2011, doi: 10.1186/1743-0003-8-25.

[17] A. M. Simon, L. J. Hargrove, B. A. Lock, and T. A. Kuiken, "A decision-based velocity ramp for minimizing the effect of misclassifications during real-time pattern recognition control," *IEEE Trans. Biomed. Eng.*, vol. 58, no. 8, pp. 2360–2368, Aug. 2011, doi: 10.1109/TBME.2011.2155063.

[18] E. J. Scheme, B. S. Hudgins, and K. B. Englehart, "Confidence-based rejection for improved pattern recognition myoelectric control," *IEEE Trans. Biomed. Eng.*, vol. 60, no. 6, pp. 1563–1570, Jun. 2013, doi: 10.1109/TBME.2013.2238939.

[19] B. Hudgins, P. Parker, and R. N. Scott, "A new strategy for multifunction myoelectric control," *IEEE Trans. Biomed. Eng.*, vol. 40, no. 1, pp. 82–94, Jan. 1993, doi: 10.1109/10.204774.

[20] G. Kanitz, C. Cipriani, and B. B. Edin, "Classification of transient myoelectric signals for the control of multi-grasp hand prostheses," *IEEE Trans. Neural Syst. Rehabil. Eng.*, vol. 26, no. 9, pp. 1756–1764, Sep. 2018, doi: 10.1109/TNSRE.2018.2861465.

[21] D. D'Accolti, F. Clemente, A. Mannini, E. Mastinu, M. Ortiz-Catalan, and C. Cipriani, "Online classification of transient EMG patterns for the control of the wrist and hand in a transradial prosthesis," *IEEE Robot. Autom. Lett.*, vol. 8, no. 2, pp. 1045–1052, Feb. 2023, doi: 10.1109/LRA.2023.3235680.

[22] D. D'Accolti, K. Dejanovic, L. Cappello, E. Mastinu, M. Ortiz-Catalan, and C. Cipriani, "Decoding of multiple wrist and hand movements using a transient EMG classifier," *IEEE Trans. Neural Syst. Rehabil. Eng.*, vol. 31, pp. 208–217, 2023, doi: 10.1109/TNSRE.2022.3218430.

[23] Y. Yamazaki, M. Suzuki, and T. Mano, "An electromyographic volley at initiation of rapid isometric contractions of the elbow," *Brain Res. Bull.*, vol. 30, nos. 1–2, pp. 181–187, Jan. 1993, doi: (10.1016/0361-9230(93)90057-i.

[24] T. W. Calvert and A. E. Chapman, "The relationship between the surface EMG and force transients in muscle: Simulation and experimental studies," *Proc. IEEE*, vol. 65, no. 5, pp. 682–689, May 1977, doi: 10.1109/PROC.1977.10547.

[25] I. J. R. Martínez, A. Mannini, F. Clemente, and C. Cipriani, "Online grasp force estimation from the transient EMG," *IEEE Trans. Neural Syst. Rehabil. Eng.*, vol. 28, no. 10, pp. 2333–2341, Oct. 2020, doi: 10.1109/TNSRE.2020.3022587.

[26] I. J. R. Martinez, A. Mannini, F. Clemente, A. M. Sabatini, and C. Cipriani, "Grasp force estimation from the transient EMG using high-density surface recordings," *J. Neural Eng.*, vol. 17, no. 1, Feb. 2020, Art. no. 016052, doi: 10.1088/1741-2552/ab673f.

[27] M. P. Mobarak, J. M. G. Salgado, R. M. Guerrero, and V. L. Dorr, "Transient state analysis of the multichannel EMG signal using Hjorth's parameters for identication of hand movements," in *Proc. ICCGI*, Jul. 2014, pp. 38–198.

[28] X. Zhang, X. Li, O. W. Samuel, Z. Huang, P. Fang, and G. Li, "Improving the robustness of electromyogram-pattern recognition for prosthetic control by a postprocessing strategy," *Frontiers Neurorobotics*, vol. 11, pp. 11–2017, Sep. 2017, doi: 10.3389/fnbot.2017.00051.

[29] S. T. P. Raghu, D. MacIsaac, and E. Scheme, "Decision-change informed rejection improves robustness in pattern recognition-based myoelectric control," *IEEE J. Biomed. Health Informat.*, vol. 27, no. 12, pp. 6051–6061, Dec. 2023, doi: 10.1109/JBHI.2023.3316599.

[30] G. Cho et al., "Characterization of signal features for real-time sEMG onset detection," *Biomed. Signal Process. Control*, vol. 84, Jul. 2023, Art. no. 104774, doi: 10.1016/j.bspc.2023.104774.

[31] N. Jiang, T. Lorrain, and D. Farina, "A state-based, proportional myoelectric control method: Online validation and comparison with the clinical state-of-the-art," *J. NeuroEng. Rehabil.*, vol. 11, no. 1, p. 110, Dec. 2014, doi: 10.1186/1743-0003-11-110.

[32] T. A. Kuiken, L. A. Miller, K. Turner, and L. J. Hargrove, "A comparison of pattern recognition control and direct control of a multiple degree-of-freedom transradial prosthesis," *IEEE J. Transl. Eng. Health Med.*, vol. 4, pp. 1–8, 2016, doi: 10.1109/JTEHM.2016.2616123.

[33] E. Gasparini et al., "LimbMATE: A versatile platform for closed-loop research in prosthetics," *IEEE Trans. Neural Syst. Rehabil. Eng.*, vol. 33, pp. 2112–2122, 2025, doi: 10.1109/TNSRE.2025.3573917.

[34] E. Scheme and K. Englehart, "A comparison of classification based confidence metrics for use in the design of myoelectric control systems," in *Proc. 37th Annu. Int. Conf. IEEE Eng. Med. Biol. Soc. (EMBC)*, Aug. 2015, pp. 7278–7283, doi: 10.1109/EMBC.2015.7320072.

[35] E. Campbell, A. Phinyomark, and E. Scheme, "Linear discriminant analysis with Bayesian risk parameters for myoelectric control," in *Proc. IEEE Global Conf. Signal Inf. Process. (GlobalSIP)*, Nov. 2019, pp. 1–5, doi: 10.1109/GlobalSIP45357.2019.8969237.

[36] M. Controzzi, F. Clemente, D. Barone, A. Ghionzoli, and C. Cipriani, "The SSSA-MyHand: A dexterous lightweight myoelectric hand prosthesis," *IEEE Trans. Neural Syst. Rehabil. Eng.*, vol. 25, no. 5, pp. 459–468, May 2017, doi: 10.1109/TNSRE.2016.2578980.

[37] M. Ortiz-Catalan, R. Brånemark, and B. Håkansson, "BioPatRec: A modular research platform for the control of artificial limbs based on pattern recognition algorithms," *Source Code for Biol. Med.*, vol. 8, no. 1, p. 11, Dec. 2013, doi: 10.1186/1751-0473-8-11.

[38] M. Ortiz-Catalan, B. Håkansson, and R. Brånemark, "Real-time and simultaneous control of artificial limbs based on pattern recognition algorithms," *IEEE Trans. Neural Syst. Rehabil. Eng.*, vol. 22, no. 4, pp. 756–764, Jul. 2014, doi: 10.1109/TNSRE.2014.2305097.

[39] N. V. Chawla, K. W. Bowyer, L. O. Hall, and W. P. Kegelmeyer, "SMOTE: Synthetic minority over-sampling technique," *J. Artif. Intell. Res.*, vol. 16, pp. 321–357, Jun. 2002.

[40] C. M. Light, P. H. Chappell, and P. J. Kyberd, "Establishing a standardized clinical assessment tool of pathologic and prosthetic hand function: Normative data, reliability, and validity," *Arch. Phys. Med. Rehabil.*, vol. 83, no. 6, pp. 776–783, Jun. 2002, doi: 10.1053/apmr.2002.32737.

[41] D. A. Bennett and M. Goldfarb, "IMU-based wrist rotation control of a transradial myoelectric prosthesis," *IEEE Trans. Neural Syst. Rehabil. Eng.*, vol. 26, no. 2, pp. 419–427, Feb. 2018, doi: 10.1109/TNSRE.2017.2682642.

[42] J. M. Hahne, M. A. Wilke, M. Koppe, D. Farina, and A. F. Schilling, "Longitudinal case study of regression-based hand prosthesis control in daily life," *Frontiers Neurosci.*, vol. 14, Jun. 2020, doi: 10.3389/fnins.2020.00600.

[43] J. Zbinden et al., "Improved control of a prosthetic limb by surgically creating electro-neuromuscular constructs with implanted electrodes," *Sci. Transl. Med.*, vol. 15, no. 704, Jul. 2023, doi: 10.1126/scitranslmed.abq3665.

[44] M. Gherardini et al., "Restoration of grasping in an upper limb amputee using the myokinetic prosthesis with implanted magnets," *Sci. Robot.*, vol. 9, no. 94, p. 3260, Sep. 2024, doi: 10.1126/scirobotics.adp3260.

[45] L. Resnik, M. Borgia, J. M. Cancio, J. Delikat, and P. Ni, "Psychometric evaluation of the Southampton hand assessment procedure (SHAP) in a sample of upper limb prosthesis users," *J. Hand Therapy*, vol. 36, no. 1, pp. 110–120, Jan. 2023, doi: 10.1016/j.jht.2021.07.003.

[46] S. G. Hart and L. E. Staveland, "Development of NASA-TLX (task load index): Results of empirical and theoretical research," in *Human Mental Workload (Advances in Psychology)*, vol. 52, P. A. Hancock and N. Meshkati, Eds., Holland, MI, USA: North-Holland, 1988, pp. 139–183, doi: (10.1016/S0166-4115(08)62386-9.

[47] L. E. Osborn et al., "Extended home use of an advanced osseointegrated prosthetic arm improves function, performance, and control efficiency," *J. Neural Eng.*, vol. 18, no. 2, Mar. 2021, Art. no. 026020, doi: 10.1088/1741-2552/abe20d.

[48] A. M. Simon and L. J. Hargrove, "A comparison of the effects of majority vote and a decision-based velocity ramp on real-time pattern recognition control," in *Proc. Annu. Int. Conf. IEEE Eng. Med. Biol. Soc.*, Aug. 2011, pp. 3350–3353, doi: 10.1109/IEMBS.2011.6090908.

[49] T. R. Farrell and R. F. Weir, "The optimal controller delay for myoelectric prostheses," *IEEE Trans. Neural Syst. Rehabil. Eng.*, vol. 15, no. 1, pp. 111–118, Mar. 2007, doi: 10.1109/TNSRE.2007.891391.

[50] C. Widehammar, A. Hiyoshi, K. Lidström Holmqvist, H. Lindner, and L. Hermansson, "Effect of multi-grip myoelectric prosthetic hands on daily activities, pain-related disability and prosthesis use compared with single-grip myoelectric prostheses: A single-case study," *J. Rehabil. Med.*, Nov. 2021, doi: 10.2340/jrm.v53.807.

[51] E. Vasluian, R. Bongers, H. Reinders-Messelink, J. Burgerhof, P. Dijkstra, and C. Sluis, "Learning effects of repetitive administration of the southampton hand assessment procedure in novice prosthetic users," *J. Rehabil. Med.*, vol. 46, no. 8, pp. 788–797, May 2014, doi: 10.2340/16501977-1827.

[52] L. Resnik, H. Huang, A. Winslow, D. L. Crouch, F. Zhang, and N. Wolk, "Evaluation of EMG pattern recognition for upper limb prosthesis control: A case study in comparison with direct myoelectric control," *J. NeuroEng. Rehabil.*, vol. 15, no. 1, p. 23, Dec. 2018, doi: 10.1186/s12984-018-0361-3.

[53] S. Amsuess et al., "Context-dependent upper limb prosthesis control for natural and robust use," *IEEE Trans. Neural Syst. Rehabil. Eng.*, vol. 24, no. 7, pp. 744–753, Jul. 2016, doi: 10.1109/TNSRE.2015.2454240.

[54] C. R. Carvalho, J. M. Fernández, A. J. del-Ama, F. Oliveira Barroso, and J. C. Moreno, "Review of electromyography onset detection methods for real-time control of robotic exoskeletons," *J. NeuroEng. Rehabil.*, vol. 20, no. 1, p. 141, Oct. 2023, doi: 10.1186/s12984-023-01268-8.

[55] Z. Zhang, C. He, and K. Yang, "A novel surface electromyographic signal-based hand gesture prediction using a recurrent neural network," *Sensors*, vol. 20, no. 14, p. 3994, 2020, doi: 10.3390/s20143994.

[56] S. Solnik, P. Rider, K. Steinweg, P. DeVita, and T. Hortobágyi, "Teager–Kaiser energy operator signal conditioning improves EMG onset detection," *Eur. J. Appl. Physiol.*, vol. 110, no. 3, pp. 489–498, Oct. 2010, doi: 10.1007/s00421-010-1521-8.

[57] S. Benatti et al., "EMG acquisition and processing for hand movement decoding on embedded systems: State of the art and challenges," *Proc. IEEE*, vol. 113, no. 3, pp. 256–286, Mar. 2025, doi: 10.1109/JPROC.2025.3581995.

[58] C. L. Chicoine, A. M. Simon, and L. J. Hargrove, "Prosthesis-guided training of pattern recognition-controlled myoelectric prosthesis," in *Proc. Annu. Int. Conf. IEEE Eng. Med. Biol. Soc.*, Aug. 2012, pp. 1876–1879, doi: 10.1109/EMBC.2012.6346318.

[59] L. Hargrove, Y. Losier, B. Lock, K. Englehart, and B. Hudgins, "A real-time pattern recognition based myoelectric control usability study implemented in a virtual environment," in *Proc. 29th Annu. Int. Conf. IEEE Eng. Med. Biol. Soc.*, Aug. 2007, pp. 4842–4845, doi: 10.1109/IEMBS.2007.4353424.

[60] E. Scheme and K. Englehart, "Training strategies for mitigating the effect of proportional control on classification in pattern recognition–based myoelectric control," *JPO J. Prosthetics Orthotics*, vol. 25, no. 2, pp. 76–83, 2013. [Online]. Available: https://journals.lww.com/jpojournal/fulltext/2013/04000/training_strategies_for_mitigating_the_effect_of.4.aspx

[61] A. T. Wang, C. D. Olsen, W. C. Hamrick, and J. A. George, "Correcting temporal inaccuracies in labeled training data for electromyographic control algorithms," in *Proc. Int. Conf. Rehabil. Robot. (ICORR)*, Sep. 2023, pp. 1–6, doi: 10.1109/ICORR58425.2023.10304728.

[62] M. Christian, C. Evan, and S. Erik, "Exploring user compliance in the training of regression-based myoelectric control," in *Proc. Myoelectric Controls Symp.*, Aug. 2024, doi: 10.57922/mec.2507.

[63] Z. Yin et al., "A wearable multisensor fusion system for neuroprosthetic hand," *IEEE Sensors J.*, vol. 25, no. 8, pp. 12547–12558, Apr. 2025, doi: 10.1109/JSEN.2025.3546214.

[64] H. E. Williams, C. S. Chapman, P. M. Pilarski, A. H. Vette, and J. S. Hebert, "Myoelectric prosthesis users and non-disabled individuals wearing a simulated prosthesis exhibit similar compensatory movement strategies," *J. NeuroEng. Rehabil.*, vol. 18, no. 1, p. 72, Dec. 2021, doi: 10.1186/s12984-021-00855-x.

[65] J. T. Belter, J. L. Segil, A. M. Dollar, and R. F. Weir, "Mechanical design and performance specifications of anthropomorphic prosthetic hands: A review," *J. Rehabil. Res. Develop.*, vol. 50, no. 5, pp. 599–618, Jul. 2013, doi: 10.1682/jrrd.2011.10.0188.